

Feasible Policy Iteration

Yujie Yang, Zhilong Zheng, Shengbo Eben Li

Abstract—Safe reinforcement learning (RL) aims to solve an optimal control problem under safety constraints. Existing *direct* safe RL methods use the original constraint throughout the learning process. They either lack theoretical guarantees of the policy during iteration or suffer from infeasibility problems. To address this issue, we propose an *indirect* safe RL method called feasible policy iteration (FPI) that iteratively uses the feasible region of the last policy to constrain the current policy. The feasible region is represented by a feasibility function called constraint decay function (CDF). The core of FPI is a region-wise policy update rule called feasible policy improvement, which maximizes the return under the constraint of the CDF inside the feasible region and minimizes the CDF outside the feasible region. This update rule is always feasible and ensures that the feasible region monotonically expands and the state-value function monotonically increases inside the feasible region. Using the feasible Bellman equation, we prove that FPI converges to the maximum feasible region and the optimal state-value function. Experiments on classic control tasks and Safety Gym show that our algorithms achieve lower constraint violations and comparable or higher performance than the baselines.

I. INTRODUCTION

Reinforcement learning (RL) has achieved promising performance on many challenging control tasks such as video games [1], board games [2], and robotics [3], and autonomous driving [4]. RL solves the optimal control policy by maximizing the expected accumulative rewards. However, in many real-world control tasks, the policy not only needs to maximize rewards but also must maintain strict safety constraints [5], [6]. Learning a policy with zero constraint violations while optimizing rewards remains a challenge for existing RL algorithms.

The essence of safe RL is to solve a constrained optimal control problem (OCP). The objective function of the constrained OCP is the expected accumulative rewards, while the constraints can take different forms. In this paper, we consider the deterministic state-wise constraint [7], [8], which requires that the state of the system always stays in a constrained set. This form of constraint widely exists in real-world control problems. For example, an autonomous vehicle must avoid collisions with surrounding vehicles, humans, and road objects at all times. Directly solving an infinite-horizon OCP with deterministic state-wise constraint is difficult because there are infinitely many constraints. This difficulty can be solved by introducing a feasibility function that aggregates the infinitely many constraints into a single one. Examples of the feasibility function include the cost value function [9], which is the discounted sum of constraints, and Hamilton-Jacobi reachability

function [10], which is the maximum constraint. Through the feasibility function, we can obtain a tractable constrained OCP with a single objective function and a single constraint.

Existing safe RL methods use constrained optimization algorithms to solve the constrained OCP, usually in an iterative manner. We call them *direct* methods because they use the original constraint throughout the iteration process. A large class of direct methods is based on the method of Lagrange multipliers, which converts a constrained problem into an unconstrained problem through the Lagrange multiplier and solves the saddle point of the Lagrangian function [11]. Chow et al. [12] alternately update the policy parameters and the Lagrange multiplier using gradient descent. Tessler et al. [13] incorporate the constraint as a penalty signal into the reward function and apply a standard actor-critic method. Ding et al. [14] update the policy parameters via natural policy gradient ascent and the Lagrange multiplier via projected sub-gradient descent. A disadvantage of these methods is that the learning process is unstable, i.e., their objective functions and constraint functions oscillate a lot [15]. This is because the Lagrange multiplier method only guarantees an optimal and constraint-satisfying policy at convergence [16] but does not provide any guarantees on either the performance or the safety of intermediate policies. Although Stooke et al. [15] propose a PID Lagrangian method to dampen the oscillation, guarantees of intermediate policies are still missing.

Another class of direct methods is based on trust region methods, which approximate the objective function and the constraint function with certain models in a region around the current solution and analytically solve the approximated problems. Achiam et al. [9] propose an algorithm called constrained policy optimization (CPO) that approximates the objective and constraint functions with affine functions in a region defined by the KL-divergence. They prove that the policy performance is lower bounded and the constraint violation is upper bounded in each iteration. A shortcoming of CPO is that the problem can become infeasible, i.e., there is no policy in the trust region that satisfies the constraint. In this case, CPO performs an update that purely decreases the constraint value, which in turn undermines the theoretical guarantees of the policy. Yu et al. [17] approximate the objective and constraint functions with quadratic functions and relax the constraint when the problem is infeasible. They prove the convergence of the algorithm but does not provide guarantees during iterations. Yang et al. [18] use the same approximations as CPO and deal with the infeasibility problem by first performing a reward improvement update and then projecting the policy back onto the constraint set. However, the lower and upper bounds become looser than those in CPO and depend on the constraint violation of the current policy, which can be large in the early stages of learning.

(Yujie Yang and Zhilong Zheng contributed equally to this work.) (Corresponding author: Shengbo Eben Li.)

The authors are with the School of Vehicle and Mobility, Tsinghua University, Beijing 100084, China (e-mail: lisb04@gmail.com).

The above direct safe RL methods either lack theoretical guarantees of the policy during iteration or suffer from infeasibility problems. To address this issue, we propose an *indirect* safe RL method that iteratively uses the feasible region of the last policy to constrain the current policy. Our method, called feasible policy iteration (FPI), solves a feasible optimization problem in each iteration and guarantees monotonic expansion of the feasible region and monotonic improvement of the state-value function. FPI adopts a three-step iteration process: policy evaluation, feasible region identification, and feasible policy improvement. In feasible region identification step, we learn a feasibility function called constraint decay function (CDF) to represent the feasible region of the current policy. In feasible policy improvement step, we use different update rules inside and outside the feasible region. Inside the feasible region, we maximize the state-value function while constraining the next state to be still feasible. Outside the feasible region, we minimize the CDF in the next state. This region-wise update rule ensures that the CDF monotonically decreases and the state-value function monotonically increases inside the feasible region. Using these two monotonicities and the feasible Bellman equation, we prove that FPI converges to the maximum feasible region and the optimal state-value function. FPI is compatible with both off-policy and on-policy RL algorithms. We propose two algorithms that combine FPI with soft actor-critic (SAC) [19] and proximal policy optimization (PPO) [20] respectively and test them on both classic control tasks and Safety Gym [21]. Experiment results show that our algorithms ensure strict safety and near-optimal performance on classic control tasks and achieve lower constraint violations and comparable or higher performance than the baselines on Safety Gym.

II. PRELIMINARIES

A. Problem formulation

We consider a deterministic Markov decision process (MDP) specified by a tuple $(\mathcal{X}, \mathcal{U}, f, r, \gamma, d_{\text{init}})$, where $\mathcal{X} \subseteq \mathbb{R}^n$ is the state space, $\mathcal{U} \subseteq \mathbb{R}^m$ is the action space, $f : \mathcal{X} \times \mathcal{U} \rightarrow \mathcal{X}$ is the dynamics model, $r : \mathcal{X} \times \mathcal{U} \rightarrow \mathbb{R}$ is the reward function, $0 < \gamma < 1$ is the discount factor, and d_{init} is the initial state distribution.

Safety is specified through state constraints, i.e., $h(x) \leq 0$, where $h : \mathcal{X} \rightarrow \mathbb{R}$ is the constraint function. The constrained set is defined as $X_{\text{Cstr}} = \{x | h(x) \leq 0\}$. The unconstrained set is defined as $\bar{X}_{\text{Cstr}} = \mathcal{X} \setminus X_{\text{Cstr}}$. An initial state drawn from d_{init} is assumed to be in X_{Cstr} with probability 1. Our aim is to find a policy $\pi : \mathcal{X} \rightarrow \mathcal{U}$ that maximizes the expected accumulative rewards under the state constraints,

$$\begin{aligned} \max_{\pi} \quad & \mathbb{E}_{x_0 \sim d_{\text{init}}(x)} \left\{ \sum_{t=0}^{\infty} \gamma^t r(x_t, u_t) \right\}, \\ \text{s.t.} \quad & h(x_t) \leq 0, t = 0, 1, \dots, \infty. \end{aligned} \quad (1)$$

B. Feasibility and optimality

The constraint function only describes the safety of a state at the current time step. To describe long-term safety, we introduce the concept of feasibility.

Definition 1. (Feasibility)

- 1) A state x is feasible if there exists a policy π , such that $h(x_t) \leq 0, t = 0, 1, \dots, \infty, x_0 = x, u_t = \pi(x_t)$.
- 2) A state x is feasible under a policy π if $h(x_t) \leq 0, t = 0, 1, \dots, \infty, x_0 = x, u_t = \pi(x_t)$.
- 3) The feasible region of π , denoted as X^π , is the set of all states that are feasible under π . The infeasible region of π is $\bar{X}^\pi = \mathcal{X} \setminus X^\pi$.
- 4) The maximum feasible region, denoted as X^* , is the set of all feasible states. The infeasible region is $\bar{X}^* = \mathcal{X} \setminus X^*$.
- 5) A policy π is feasible if $X^\pi = X^*$. The set of all feasible policies is denoted as Π^* .

The feasible region of a policy is the maximum region where it can be safely applied, i.e., where the constraint is always satisfied. To achieve a high performance, we want this region to be as large as possible. In particular, we want it to equal the maximum feasible region. Also, we want to maximize the state-value function of the policy. We call these two properties feasible optimality, which is defined as follows.

Definition 2. (Feasible optimality) $V : X^* \rightarrow \mathbb{R}$ is the feasible optimal state-value function if for all $x \in X^*$,

$$V(x) = \max_{\pi \in \Pi^*} V^\pi(x). \quad (2)$$

We denote the feasible optimal state-value function as V^* . A policy π is a feasible optimal policy if $\pi \in \Pi^*$ and for all $x \in X^*$, $V^\pi(x) = V^*(x)$.

III. FEASIBLE POLICY ITERATION

In this section, we introduce our indirect safe RL method called feasible policy iteration (FPI). First, we propose a feasibility function called constraint decay function (CDF) for representing the feasible region of a given policy. Then, we detail the core step of our algorithm, feasible policy improvement, and prove two monotonic properties of the policy. Next, we present the overall FPI algorithm and prove its convergence. Finally, we introduce some practical implementations under function approximations.

A. Constraint decay function

Definition 3. (Constraint decay function) The constraint decay function of a policy π , $F^\pi : \mathcal{X} \rightarrow [0, 1]$, is defined as

$$F^\pi(x) = \gamma^{N^\pi(x)}, \quad (3)$$

where $0 < \gamma < 1$ is the discount factor and $N^\pi(x)$ is the number of time steps to constraint violation starting from x under π .

For a state x , if $x \in \bar{X}_{\text{Cstr}}$, then $N^\pi(x) = 0$. If $x \in X^\pi$, then $N^\pi(x) = \infty$. If $x \in \bar{X}^\pi \cap X_{\text{Cstr}}$, then $0 < N^\pi(x) < \infty$. Thus, the zero-level set of F^π represents the feasible region of π , i.e., $X^\pi = \{x | F^\pi(x) = 0\}$. The CDF satisfies the following self-consistency condition.

Theorem 1. (Self-consistency condition) For all $x \in \mathcal{X}$,

$$F^\pi(x) = c(x) + (1 - c(x))\gamma F^\pi(x'), \quad (4)$$

where $c(x) = \mathbf{1}_{\bar{X}_{\text{Cstr}}}(x)$ and $x' = f(x, \pi(x))$.

Proof. For all $x \in X^\pi$, $c(x) = 0$, $N^\pi(x) = N^\pi(x') = \infty$, $F^\pi(x) = F^\pi(x') = 0$, (4) holds. For all $x \in \bar{X}_{\text{Cstr}}$, $c(x) = 1$, $N^\pi(x) = 0$, $F^\pi(x) = 1$, (4) holds. For all $x \in \bar{X}^\pi \cap X_{\text{Cstr}}$, $c(x) = 0$, $N^\pi(x) = N^\pi(x') + 1$, $F^\pi(x) = \gamma^{N^\pi(x)} = \gamma \cdot \gamma^{N^\pi(x')} = \gamma F^\pi(x')$, (4) holds. Thus, for all $x \in \mathcal{X}$, (4) holds. \square

The self-consistency condition induces a contraction mapping, which enables us to compute the CDF using an iterative method.

Theorem 2. (Contraction mapping) Define the constraint decay operator D^π as

$$(D^\pi F)(x) = c(x) + (1 - c(x))\gamma F(x'). \quad (5)$$

D^π is a contraction mapping under the infinity norm, i.e., there exists a constant $\kappa \in [0, 1)$, such that for all $F_1, F_2 : \mathcal{X} \rightarrow [0, 1]$, $\|D^\pi F_1 - D^\pi F_2\|_\infty \leq \kappa \|F_1 - F_2\|_\infty$.

Proof. For all $x \in \mathcal{X}$,

$$\begin{aligned} |D^\pi F_1(x) - D^\pi F_2(x)| &= |(1 - c(x))\gamma(F_1(x') - F_2(x'))| \\ &\leq \gamma|F_1(x') - F_2(x')| \\ &\leq \gamma\|F_1 - F_2\|_\infty. \\ \|D^\pi F_1 - D^\pi F_2\|_\infty &= \sup_x |D^\pi F_1(x) - D^\pi F_2(x)| \\ &\leq \gamma\|F_1 - F_2\|_\infty. \end{aligned}$$

Since $\gamma \in (0, 1)$, D^π is a contraction mapping. \square

According to Banach's fixed-point theorem, D^π admits a unique fixed point, which can be found by iteratively applying D^π starting from an arbitrary F .

Proposition 1. F^π is the unique fixed point of D^π .

Proposition (1) can be proved directly by the self-consistency condition (4). Let F_k be the CDF in the k -th iteration, $k = 0, 1, \dots, \infty$. The update rule for F_k is

$$F_{k+1} = D^\pi F_k. \quad (6)$$

According to Theorem 2 and Proposition 1, F_k converges to F^π . We call this algorithm feasible region identification.

B. Feasible policy improvement

Feasible policy improvement is the core step of FPI. It updates the policy to obtain a larger feasible region and a higher state-value function. In each iteration, we apply different update rules to states inside and outside the feasible region of the last policy, which we denote as π_k . Inside the feasible region, we solve a constrained optimization problem that maximizes the reward plus the state-value function of π_k in the next state under the constraint that the next state is still feasible under π_k , i.e., for all $x \in X^{\pi_k}$,

$$\begin{aligned} \pi_{k+1}(x) &= \arg \max_u r(x, u) + \gamma V^{\pi_k}(x') \\ \text{s.t. } &F^{\pi_k}(x') = 0, \end{aligned} \quad (7)$$

where $x' = f(x, u)$. Outside the feasible region, problem (7) may be infeasible so we turn to solve an unconstrained

optimization problem that minimizes the feasibility function of π_k in the next state, i.e., for all $x \in \bar{X}^{\pi_k}$,

$$\pi_{k+1}(x) = \arg \min_u F^{\pi_k}(x'). \quad (8)$$

The following theorem states that the new policy π_{k+1} obtained by (7) and (8) is 'more feasible' than the old policy π_k .

Theorem 3. (Feasibility enhancement) The CDF of π_{k+1} is not greater than that of π_k , i.e., for all $x \in \mathcal{X}$, $F^{\pi_{k+1}}(x) \leq F^{\pi_k}(x)$.

Proof. According to (8), for all $x \in \bar{X}^{\pi_k}$, $F^{\pi_k}(f(x, \pi_k(x))) \geq F^{\pi_k}(f(x, \pi_{k+1}(x)))$. According to (7), for all $x \in X^{\pi_k}$, $F^{\pi_k}(f(x, \pi_{k+1}(x))) = 0$. Thus, for all $x \in \mathcal{X}$,

$$\begin{aligned} F^{\pi_k}(x) &= c(x) + (1 - c(x))\gamma F^{\pi_k}(f(x, \pi_k(x))) \\ &\geq c(x) + (1 - c(x))\gamma F^{\pi_k}(f(x, \pi_{k+1}(x))). \end{aligned}$$

Let $\{x_t\}_{t=0}^\infty$ be the state trajectory under π_{k+1} , where $x_0 = x$. We denote $c(x_t)$ as c_t for simplicity.

$$\begin{aligned} F^{\pi_k}(x) &\geq c_0 + (1 - c_0)\gamma F^{\pi_k}(x_1) \\ &\geq c_0 + (1 - c_0)\gamma(c_1 + (1 - c_1)\gamma F^{\pi_k}(x_2)) \\ &\vdots \\ &\geq c_0 + \gamma(1 - c_0)c_1 + \gamma^2(1 - c_0)(1 - c_1)c_2 + \dots \\ &= \sum_{t=0}^{\infty} \gamma^t \prod_{s=0}^{t-1} (1 - c_s) c_t \\ &= \gamma^{N^{\pi_{k+1}}(x)} \\ &= F^{\pi_{k+1}}(x). \end{aligned}$$

\square

A corollary of Theorem 3 is that the feasible region monotonically expands.

Corollary 1. (Monotonic expansion) The feasible region of π_{k+1} is at least as large as that of π_k , i.e., $X^{\pi_{k+1}} \subseteq X^{\pi_k}$.

Proof. $\forall x \in X^{\pi_k}$, $F^{\pi_{k+1}}(x) \leq F^{\pi_k}(x) = 0$, $x \in X^{\pi_{k+1}}$. \square

The following theorem states that the new policy π_{k+1} obtained by (7) and (8) is better in performance than the old policy π_k in the feasible region of π_k .

Theorem 4. (Feasible policy improvement) The state-value function of π_{k+1} is not less than that of π_k in the feasible region of π_k , i.e., for all $x \in X^{\pi_k}$, $V^{\pi_{k+1}}(x) \geq V^{\pi_k}(x)$.

Proof. For all $x \in X^{\pi_k}$, let $U^{\pi_k}(x) = \{u | F^{\pi_k}(x') = 0\}$. We have $\pi_k(x), \pi_{k+1}(x) \in U^{\pi_k}(x)$. According to (7),

$$\begin{aligned} V^{\pi_k}(x) &= r(x, \pi_k(x)) + \gamma V^{\pi_k}(f(x, \pi_k(x))) \\ &\leq r(x, \pi_{k+1}(x)) + \gamma V^{\pi_k}(f(x, \pi_{k+1}(x))). \end{aligned}$$

Let $\{x_t\}_{t=0}^\infty$ be the state trajectory under π_{k+1} , where $x_0 = x$. We denote $r(x_t, \pi_{k+1}(x_t))$ as r_t for simplicity.

$$\begin{aligned} V^{\pi_k}(x) &\leq r_0 + \gamma V^{\pi_k}(x_1) \\ &\leq r_0 + \gamma r_1 + \gamma^2 V^{\pi_k}(x_2) \\ &\vdots \\ &\leq r_0 + \gamma r_1 + \gamma^2 r_2 + \dots \\ &= \sum_{t=0}^\infty \gamma^t r_t \\ &= V^{\pi_{k+1}}(x). \end{aligned}$$

□

C. Feasible policy iteration

Our proposed algorithm, feasible policy iteration (FPI), alternates three steps: policy evaluation, feasible region identification, and feasible policy improvement. The policy evaluation step computes the state-value function of the current policy and is the same as that in standard policy iteration. The pseudo-code of FPI is shown in Algorithm 1.

Algorithm 1: Feasible policy iteration (FPI)

Input: initial policy π_0 .
for each iteration k **do**
 Compute V^{π_k} using policy evaluation;
 Compute F^{π_k} using feasible region identification;
 for each state $x \in X^{\pi_k}$ **do**
 $\pi_{k+1}(x) = \arg \max_u r(x, u) + \gamma V^{\pi_k}(x')$,
 s.t. $F^{\pi_k}(x') = 0$;
 end
 for each state $x \in \bar{X}^{\pi_k}$ **do**
 $\pi_{k+1}(x) = \arg \min_u F^{\pi_k}(x')$;
 end
end

To prove the convergence of Algorithm 1, we first give the necessary and sufficient condition of feasible optimality, which is the feasible Bellman equation.

Theorem 5. (Feasible optimality condition) V is the feasible optimal state-value function if and only if it satisfies the feasible Bellman equation, i.e., for all $x \in X^*$,

$$V(x) = \max_{u \in U^*(x)} r(x, u) + \gamma V(x'), \quad (9)$$

where $U^*(x) = \{u | x' \in X^*\}$ and $x' = f(x, u)$.

Proof. The feasible Bellman operator,

$$(B^*V)(x) = \max_{u \in U^*(x)} r(x, u) + \gamma V(x'),$$

is a contraction mapping under the infinity norm. This can be proved in a similar way to Theorem 2. According to Banach's fixed-point theorem, B^* has a unique fixed point, which is the solution to (9). Thus, we only need to prove that the feasible

optimal state-value function is the solution to (9). For all $x \in X^*$, let $x_0 = x$,

$$\begin{aligned} V^*(x) &= \max_{\pi \in \Pi^*} V^\pi(x) \\ &= \max_{\substack{u_t \in U^*(x_t) \\ t=0,1,\dots,\infty}} \sum_{t=0}^\infty \gamma^t r(x_t, u_t) \\ &= \max_{u \in U^*(x)} r(x, u) + \max_{\substack{u_t \in U^*(x_t) \\ t=1,2,\dots,\infty}} \sum_{t=1}^\infty \gamma^t r(x_t, u_t) \\ &= \max_{u \in U^*(x)} r(x, u) + \gamma \max_{\pi \in \Pi^*} V^\pi(x') \\ &= \max_{u \in U^*(x)} r(x, u) + \gamma V^*(x'). \end{aligned}$$

□

The following theorem shows that Algorithm 1 converges to the feasible optimal policy.

Theorem 6. (Convergence of FPI) If for all $x \in \mathcal{X}$, $F^{\pi_k}(x) = F^{\pi_{k+1}}(x)$, and for all $x \in X^*$, $V^{\pi_k}(x) = V^{\pi_{k+1}}(x)$, then both π_k and π_{k+1} are feasible optimal policies.

Proof. First, we prove that both π_k and π_{k+1} are feasible policies. For all $x \in \bar{X}^{\pi_k}$ and $u \in \mathcal{U}$,

$$\begin{aligned} F^{\pi_{k+1}}(f(x, \pi_{k+1}(x))) &= F^{\pi_k}(f(x, \pi_{k+1}(x))) \\ &= \arg \min_u F^{\pi_k}(f(x, u)) \\ &\leq F^{\pi_k}(f(x, u)) \\ &= F^{\pi_{k+1}}(f(x, u)). \end{aligned}$$

For all $x \in X^{\pi_k}$ and $u \in \mathcal{U}$,

$$\begin{aligned} F^{\pi_{k+1}}(f(x, \pi_{k+1}(x))) &= F^{\pi_k}(f(x, \pi_{k+1}(x))) \\ &= 0 \leq F^{\pi_{k+1}}(f(x, u)). \end{aligned}$$

Thus, for all $x \in \mathcal{X}$ and $u \in \mathcal{U}$, $F^{\pi_{k+1}}(f(x, \pi_{k+1}(x))) \leq F^{\pi_{k+1}}(f(x, u))$. For all $x \in X^*$, there exists a sequence of actions $\{u_t\}_{t=0}^\infty$ such that the resulting state trajectory $\{x_t\}_{t=0}^\infty$ satisfies $x_t \in X^*$, $t = 0, 1, \dots, \infty$, $x_0 = x$.

$$\begin{aligned} F^{\pi_{k+1}}(x) &= c(x) + (1 - c(x))\gamma F^{\pi_{k+1}}(f(x, \pi_{k+1}(x))) \\ &\leq \gamma F^{\pi_{k+1}}(f(x_0, u_0)) = \gamma F^{\pi_{k+1}}(x_1) \\ &\vdots \\ &\leq \gamma^n F^{\pi_{k+1}}(x_n) \leq \gamma^n. \end{aligned}$$

Take the limits of both sides as $n \rightarrow \infty$,

$$F^{\pi_{k+1}}(x) = \lim_{n \rightarrow \infty} F^{\pi_{k+1}}(x) \leq \lim_{n \rightarrow \infty} \gamma^n = 0.$$

This indicates that $x \in X^{\pi_{k+1}}$. Thus, $X^* \subseteq X^{\pi_{k+1}}$. Also, $X^{\pi_{k+1}} \subseteq X^*$ by definition. Thus, $X^{\pi_{k+1}} = X^*$. Since $F^{\pi_k}(x) = F^{\pi_{k+1}}(x)$, $X^{\pi_k} = X^{\pi_{k+1}} = X^*$.

Second, we prove that both V^{π_k} and $V^{\pi_{k+1}}$ are solutions to (9). For all $x \in X^*$, $U^{\pi_k}(x) = \{u | F^{\pi_k}(x') = 0\} = \{u | x' \in X^*\} = U^*(x)$,

$$\begin{aligned} V^{\pi_{k+1}}(x) &= r(x, \pi_{k+1}(x)) + \gamma V^{\pi_{k+1}}(f(x, \pi_{k+1}(x))) \\ &= r(x, \pi_{k+1}(x)) + \gamma V^{\pi_k}(f(x, \pi_{k+1}(x))) \\ &= \max_{u \in U^{\pi_k}(x)} r(x, u) + \gamma V^{\pi_{k+1}}(x') \\ &= \max_{u \in U^*(x)} r(x, u) + \gamma V^{\pi_{k+1}}(x'). \end{aligned}$$

Since $V^{\pi_k} = V^{\pi_{k+1}}$, both of them are solutions to (9). Thus, both π_k and π_{k+1} are feasible optimal policies. \square

D. Practical implementations

To deal with problems with continuous state spaces, we use a neural network with parameters ϕ and a sigmoid output activation function to approximate the CDF. We use a cross-entropy loss for optimizing the CDF, in which the label is the right hand side of (6). The output value $F_\phi(x) \in (0, 1)$, $\forall x \in \mathcal{X}$, so the feasible region cannot be represented by $\{x | F_\phi(x) = 0\}$. To deal with this problem, we introduce a feasibility threshold $0 < p < 1$, and use the following two sets,

$$X^F = \{x | F_\phi(x) < p\}, \quad \bar{X}^F = \{x | F_\phi(x) \geq p\}, \quad (10)$$

to represent feasible and infeasible regions, respectively. In each iteration, we solve a inequality constrained optimization problem in the feasible region, i.e., for all $x \in X^{\pi_k}$,

$$\begin{aligned} \max_u \quad & r(x, u) + \gamma V^{\pi_k}(x') \\ \text{s.t.} \quad & F^{\pi_k}(x') \leq p. \end{aligned} \quad (11)$$

The initial point of (11), which is the policy from the last iteration π_k , is a feasible solution, i.e., $F^{\pi_k}(f(x, \pi_k(x))) < p$. This allows us to use the interior point method to solve (11). We add a logarithm barrier function of the constraint to the objective function and remove the constraint,

$$\max_u \quad r(x, u) + \gamma V^{\pi_k}(x) + 1/t \cdot \log(p - F^{\pi_k}(x')). \quad (12)$$

We increase t by a factor every several number of iterations. As $t \rightarrow \infty$, the solution to (12) approaches the solution to (11). Compared with other constrained optimization methods such as the dual ascent, the advantage of the interior point method is that its intermediate solutions in all iterations are feasible. This ensures that the monotonic expansion property of the feasible region is preserved.

IV. COMBINATION WITH RL ALGORITHMS

Feasible policy iteration (FPI) is compatible with both off-policy and on-policy RL algorithms. In this section, we combine FPI with two mainstream RL algorithms. The first is soft actor-critic (SAC) [19], an off-policy RL algorithm, and the second is proximal policy optimization (PPO) [20], an on-policy RL algorithm.

A. Combination with soft actor-critic

We denote this algorithm as FPI-SAC, which learns an action CDF network G_ϕ , two Q networks $Q_{\omega_1}, Q_{\omega_2}$, and a policy network π_θ . The action CDF G takes the current state and action as input and outputs the CDF value of the next state, i.e., $G(x, u) = F(f(x, u))$. The loss function of the action CDF network is

$$\begin{aligned} L_G(\phi) &= \mathbb{E}_{(x, u, c, x') \sim D} \{\text{CE}(y_G, G_\phi(x, u))\}, \\ y_G &= c + (1 - c)\gamma G_{\bar{\phi}}(x', u'), \end{aligned} \quad (13)$$

where CE is the cross-entropy loss, i.e., $\text{CE}(y, p) = -(y \log p + (1 - y) \log(1 - p))$, $\bar{\phi}$ is the parameters of the target

action CDF network, and $u' \sim \pi_\theta(\cdot | x')$. The loss functions of the Q networks are,

$$\begin{aligned} L_Q(\omega_i) &= \mathbb{E}_{(x, u, r, x') \sim D} \{(y_Q - Q_{\omega_i}(x, u))^2\}, \\ y_Q &= r + \gamma \left(\min_{j \in \{1, 2\}} Q_{\bar{\omega}_j}(x', u') - \alpha \log \pi_\theta(u' | x') \right), \end{aligned} \quad (14)$$

where $i \in \{1, 2\}$, $\bar{\omega}_j$ are the parameters of the target Q networks, and α is the temperature. The policy loss in a feasible state is

$$\begin{aligned} l_f(x) &= l_r(x) - 1/t \cdot \log(p - G_\phi(x, u)), \\ l_r(x) &= \alpha \log \pi_\theta(u | x) - \min_{i \in \{1, 2\}} Q_{\omega_i}(x, u), \end{aligned}$$

where $u \sim \pi_\theta(\cdot | x)$. The policy loss in an infeasible state is

$$l_i(x) = G_\phi(x, u).$$

The total policy loss is

$$\begin{aligned} L_\pi(\theta) &= \mathbb{E}_{x \sim D} \{m(x)l_f(x) + (1 - m(x))l_i(x)\}, \\ m(x) &= I(G_\phi(x, u) < p), \end{aligned} \quad (15)$$

where I is the indicator function, i.e., $I(S) = 1$ if S is true else 0.

B. Combination with proximal policy optimization

We denote this algorithm as FPI-PPO, which learns a CDF network F_ϕ , a value network V_ω , and a policy network π_θ . PPO computes value loss and policy loss using generalized advantage estimation (GAE) [22]. We propose a similar method for computing the loss functions in FPI-PPO. For any state $x \in \mathcal{X}$, let $\tau = \{(x_t, u_t, r_t, c_t)\}_{t=0}^\infty$ be the trajectory under π_θ , where $x_0 = x$. The k -step ($k \geq 1$) temporal difference (TD) residual of the CDF is

$$\hat{H}_k(x) = -F(x_0) + \sum_{t=0}^{k-1} C_{t-1} c_t \gamma^t + C_{k-1} \gamma^k F(x_k) \quad (16)$$

where $C_t = \prod_{s=0}^t (1 - c_s)$. The GAE of the CDF is

$$\hat{H}(x) = (1 - \lambda) \sum_{k=1}^\infty \lambda^{k-1} \hat{H}_k(x) = \sum_{t=0}^\infty (\gamma \lambda)^t C_{t-1} \hat{H}_1(x_t). \quad (17)$$

The loss function of the CDF network is

$$\begin{aligned} L_F(\phi) &= \mathbb{E}_{\tau \sim D} \{\text{CE}(y_F, F_\phi(x))\}, \\ y_F &= \hat{H}(x) + F_\phi(x), \end{aligned} \quad (18)$$

where the gradient of y_F is detached. The loss function of the value network is

$$\begin{aligned} L_V(\omega) &= \mathbb{E}_{\tau \sim D} \{(y_V - V_\omega(x))^2\}, \\ y_V &= \hat{A}(x) + V_\omega(x), \end{aligned} \quad (19)$$

where \hat{A} is the GAE of the state-value function and the gradient of y_V is detached. The constraint of the policy in a feasible state is

$$F_\phi(x) + r_\theta(x) \hat{H}(x) \leq p,$$

where $r_\theta(x) = \pi_\theta(u|x)/\pi_{\theta_{\text{old}}}(u|x)$ is the importance sampling ratio and $u \sim \pi_{\theta_{\text{old}}}(\cdot|x)$. The policy loss in a feasible state is

$$l_f(x) = l_r(x) - 1/t \cdot \log(p - (F_\phi(x) + r_\theta(x)\hat{H}(x))),$$

$$l_r(x) = -\min(r_\theta(x)\hat{A}(x), \text{clip}(r_\theta(x), 1 - \epsilon, 1 + \epsilon)\hat{A}(x)).$$

The policy loss in an infeasible state is

$$l_i(x) = r_\theta(x)\hat{H}(x).$$

The total policy loss is

$$L_\pi(\theta) = \mathbb{E}_{\tau \sim D} \{m(x)l_f(x) + (1 - m(x))l_i(x)\}, \quad (20)$$

$$m(x) = I(F_\phi(x) + r_\theta(x)\hat{H}(x) < p).$$

V. EXPERIMENTS

We seek to answer the following questions through our experiments:

- 1) Can FPI-SAC and FPI-PPO achieve monotonic feasible region expansion and performance improvement, and eventually converge to the maximum feasible region?
- 2) Compared to those *direct* algorithms based on the method of Lagrange multipliers, do FPI-SAC and FPI-PPO demonstrate a more stable during-training performance?
- 3) Do FPI-SAC and FPI-PPO outperform the *direct* algorithms in terms of both safety and optimality?

With regard to (1), we test our proposed method on four classic control tasks where the dynamics are simple and known, and thus the ground-truth maximum feasible regions are available. To answer (2) and (3), we compare the algorithms on four high-dimensional robot navigation tasks in Safety Gym [21], which are much more complicated and challenging.

Baselines. The baselines for comparison include both classes of *direct* methods for constrained policy optimization mentioned in Section I. Constrained policy optimization (**CPO**) is a representative of the trust-region-based methods, which extends trust region policy optimization [23] to CMDPs, while SAC Lagrangian (**SAC-Lag**) [24] and PPO Lagrangian (**PPO-Lag**) [21] are the Lagrangian-based counterparts of FPI-SAC and FPI-PPO, respectively.

A. Classic control tasks

1) *Task description:* The four classic control tasks include: (1) Adaptive Cruise Control (ACC); (2) Lane Keeping (LK); (3) Pendulum; (4) Quadrotor. In order to avoid confusion in symbols, in this section, we mark the state and action in bold to emphasize that they are vectors.

a) *ACC:* The goal of ACC is to control the following vehicle to converge to and maintain a fixed distance with respect to a leading vehicle moving in a uniform motion. Both following and leading vehicles are modeled as point masses moving in a straight line. The dynamics of the system is

$$\begin{pmatrix} \dot{x}_1 \\ \dot{x}_2 \end{pmatrix} = \begin{pmatrix} x_2 \\ 0 \end{pmatrix} + \begin{pmatrix} 0 \\ -1 \end{pmatrix} \mathbf{u}, \quad (21)$$

where $\mathbf{x} = [x_1, x_2]^\top \triangleq [\Delta s, \Delta v]^\top$, with Δs and Δv standing for the relative position and velocity between the two vehicles,

respectively, and $\mathbf{u} \triangleq [a]$ is the acceleration of the following vehicle.

The reward function is defined as

$$r(\mathbf{x}, \mathbf{u}) = -0.001\Delta s^2 - 0.01\Delta v^2 - a^2, \quad (22)$$

and the constraint function is

$$h(\mathbf{x}) = |\Delta s| - \Delta s_{\max}, \quad (23)$$

which, since a large acceleration is penalized in (22), will be violated by a performance-only policy.

b) *LK:* This task aims to keep a vehicle running in a straight line, i.e., having near-zero state $\mathbf{x} \triangleq [y, \varphi, v, \omega]^\top$, where y, φ, v, ω are vertical position, yaw angle, lateral velocity, and yaw rate, respectively. The vehicle follows a 2-Degree-of-Freedom (DoF) bicycle model [25], where its longitudinal velocity is a constant, and the only action is steering angle, i.e. $\mathbf{u} \triangleq [\delta]$.

The reward function penalizes stabilization errors and aggressive behaviour:

$$r(\mathbf{x}, \mathbf{u}) = -0.01y^2 - 0.01\varphi^2 - v^2 - \omega^2 - \delta^2, \quad (24)$$

and the constraint function is

$$h(\mathbf{x}) = |y| - L/2, \quad (25)$$

where L is the width of the lane.

c) *Pendulum:* The goal of Pendulum is to apply torque τ on an one-end-fixed pendulum to swing it into an upright position (see Fig. 1(a)). The state $\mathbf{x} \triangleq [\theta, \dot{\theta}]^\top$ consists of the pendulum's angle w.r.t. vertical θ and angular velocity $\dot{\theta}$ and the action is $\mathbf{u} \triangleq [\tau]$. It comes from the popular benchmark Gymnasium [26], with some slight changes in the reward function:

$$r(\mathbf{x}, \mathbf{u}) = -0.1\theta^2 - 0.01\dot{\theta}^2 - \tau^2, \quad (26)$$

and an additional constraint on the angle:

$$h(\mathbf{x}) = |\theta| - \theta_{\max} \leq 0. \quad (27)$$

d) *Quadrotor:* Different to the above-mentioned stabilization tasks, Quadrotor is a trajectory tracking task comes from safe-control-gym [27], where a 2D quadrotor is required to follow a circular trajectory in the vertical plane while keeping the vertical position in a certain range. Fig. 1(b) gives a schematic of this environment. The state of the system is $\mathbf{x} \triangleq [x, \dot{x}, z, \dot{z}, \theta, \dot{\theta}]^\top$, where (x, z) is the position of the quadrotor on xz -plane, and θ is the pitch angle. The action of the system is $\mathbf{u} \triangleq [T_1, T_2]^\top$, including the thrusts generated by two pairs of motors.

The goal is to minimize the tracking error with minimal efforts:

$$r(\mathbf{x}, \mathbf{u}) = -\|[x - x_{\text{ref}}, z - z_{\text{ref}}]\|_2^2 - 0.1\dot{\theta}^2 - \dot{\theta}^2 - 0.1(T_1 - T_0)^2 - 0.1(T_2 - T_0)^2, \quad (28)$$

where $(x_{\text{ref}}, z_{\text{ref}})$ is the reference position the quadrotor is supposed to be at, and T_0 is the thrust needed for balancing the gravity. The reference position moves along a circle

TABLE I
 R_{vio} AND R_{norm} ON FOUR CLASSIC CONTROL TASKS.

	ACC		LK		Pendulum		Quadrotor	
	R_{vio}	R_{norm}	R_{vio}	R_{norm}	R_{vio}	R_{norm}	R_{vio}	R_{norm}
SAC-Lag	0	0.9942	0	0.9970	0	0.9980	0	0.9980
FPI-SAC (ours)	0	0.9996	0	0.9980	0	0.9988	0	0.9995
PPO-Lag	0.0417	0.9805	0.0870	0.9784	0	0.9667	1	0.0842
FPI-PPO (ours)	0	0.9624	0	0.9812	0	0.9942	0	0.9997
CPO	0	0.9296	1	0.8031	0	0.8449	0	0.9995
MPC w/o cstr.	0.2083	1.0051	0.4348	1.0021	0.1739	1.0113	1	1.0003

¹ MPC w/o cstr. means applying MPC controller without considering the constraint.

$x^2 + z^2 = 0.5^2$ with a constant angular velocity, but the constraint function is

$$h(\mathbf{x}) = \begin{bmatrix} |z| - z_{\max} \\ |\theta| - \theta_{\max} \\ \|[x - x_{\text{ref}}, z - z_{\text{ref}}]\|_2 - err_{\max} \end{bmatrix} \leq 0, \quad (29)$$

restricting the quadrotor to stay in a rectangular area.

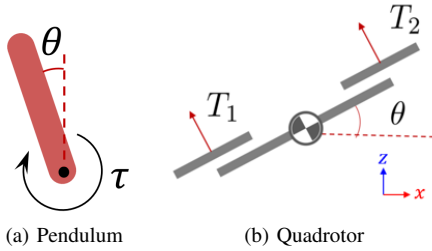


Fig. 1. Schematics of the Pendulum and the 2D quadrotor environments.

2) *Metrics*: Since the dynamics of the four classic control tasks are available, we implemented a controller based on Model Predictive Control (MPC), which computes an action sequence in an receding-horizon-control manner. Having an access to an accurate model and a long-enough prediction horizon, an MPC controller is able to yield an approximately optimal solution. We compare the five algorithms with the MPC controller acting as a performance upper bound.

The evaluation metrics includes constraint violation ratio

$$R_{vio} = \frac{N_{vio}}{N} \quad (30)$$

and average normalized return

$$R_{norm} = \frac{R_{alg} - R_{base}}{R_{MPC} - R_{base}}, \quad (31)$$

where N_{vio} is the number of episodes where the constraint was violated, N is the total number of episodes, R_{alg} , R_{base} and R_{MPC} are the average return of a certain algorithm, a random policy and an MPC controller, respectively.

3) *Results*: The R_{vio} and R_{norm} of the five algorithms on four classic control tasks are listed in Table I. We group SAC-Lag and FPI-SAC into one interval and PPO-Lag and FPI-PPO into another, to better compare our proposed methods with their corresponding counterpart. The best results in each group are showed in bold. Note that CPO is listed separately, but it won't change the best results in either group if we had put it in

that group. Note also that we further apply the MPC controller on the four tasks without considering the constraints, so as to show the effectiveness of them. Results indicate that both FPI-SAC and FPI-PPO achieve zero constraint violation on all the four tasks, and outperform their corresponding counterparts and CPO in terms of return on almost all tasks.

To show the monotonic expansion of the feasible region and monotonic improvement of the state-value function, we take FPI-SAC as an instance and plot some intermediate results during the training, as shown in Fig. 2. The state values are presented as heat maps. The maximum feasible regions and the policy's feasible regions are outlined with black lines and green lines, respectively. In all tasks, FPI-SAC demonstrates monotonicity in terms of both feasible region and state value, and the feasible regions gradually converge to the maximum feasible regions. Note that the initial state values in Fig. 2(b) and 2(c) are high only because the value networks are initialized to produce near-zero outputs and haven't acquired to give the true values at this early stage.

B. Safety Gym benchmark

1) *Task description*: To further test the performance of our proposed methods on complex tasks, We choose four safety-critical control tasks in Safety Gym [21]: PointGoal, CarGoal, PointPush and CarPush.

a) *PointGoal & CarGoal*: PointGoal and CarGoal are two robot navigation tasks, the aims of which are to control the robot (in red) to reach a goal (in green) while avoiding hazards (in blue), as shown in Fig. 3(a) and 3(b). There are 8 hazards with a radius of 0.2 and a goal with a radius of 0.3. The state includes the velocity of the robot, the position of the goal, and LiDAR point clouds of the hazards. The control inputs of the robots are the torques of their motors, controlling the motion of moving forward and turning for a Point robot, and left and right wheel for a Car robot.

b) *PointPush & CarPush*: PointPush and CarPush are similar to the last two tasks, except that the robots are trying to push a box (in yellow) to the goal, as shown in Fig. 3(c) and 3(d). There are 4 hazards with a radius of 0.1, a goal with a radius of 0.3. The state further includes the position of the box.

2) *Metrics*: We evaluate all algorithms with two metrics: average episode cost and average episode return, which are the average sum of costs and rewards in an episode, respectively.

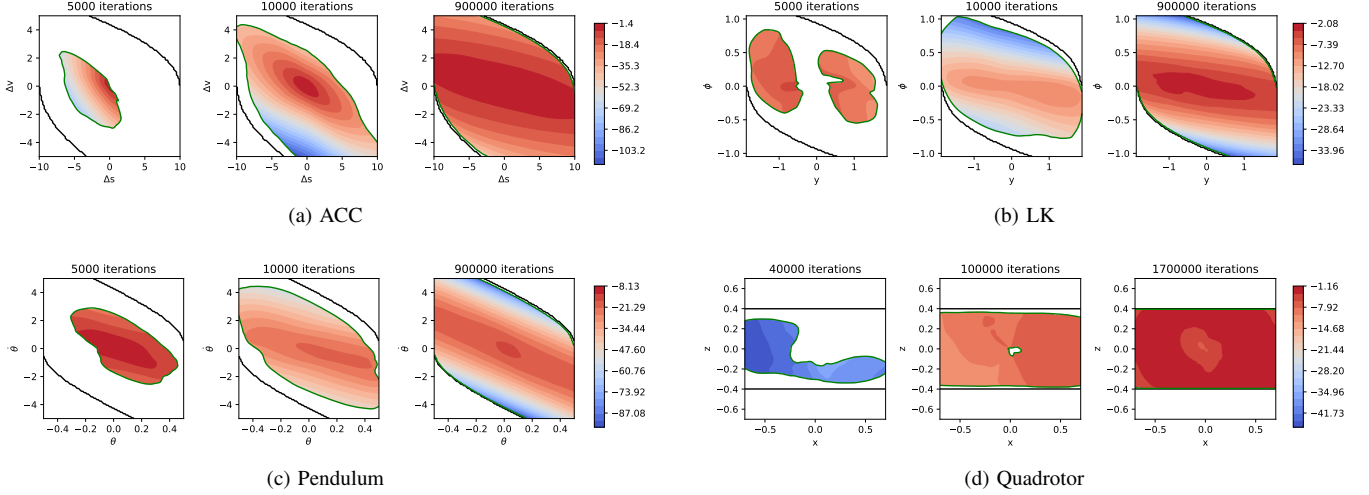


Fig. 2. Heat maps and zero-sublevel sets of the feasibility functions on four classic control tasks. The heat maps correspond to the state values. The black lines are boundaries of the maximum feasible regions, while the green ones around the coloured regions are boundaries of zero contours of the feasibility functions.

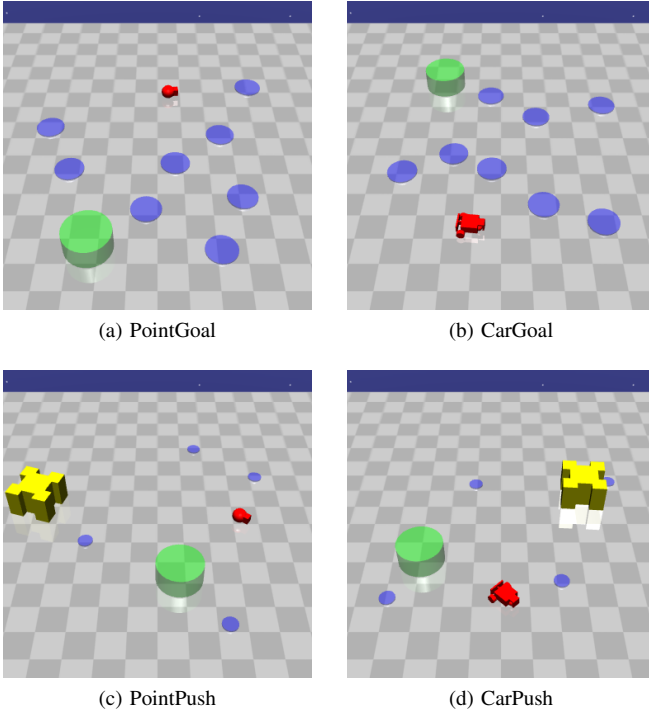


Fig. 3. Snapshots of four safety gym tasks.

3) *Results*: The training curves are shown in Fig. 4. Results show that FPI-SAC and FPI-PPO achieve near-zero constraint violations on all tasks. In comparison, CPO acts highly unsafely on all tasks except CarPush, so does SAC-Lag on two Point robot tasks, which indicates the impacts of CPO’s infeasibility problem and Lagrange multiplier method’s lack of guarantee on constraint satisfaction. In addition, FPI-SAC and FPI-PPO achieve comparable or higher performance than their corresponding counterparts and CPO on all tasks. Note that although PPO-Lag also performs great on all tasks in terms of safety, its average episode returns on two Point robot

tasks are relatively low. Note also how the curves of SAC-Lag and PPO-Lag oscillate or even become worse during training, demonstrating the instability of Lagrange multiplier method.

VI. CONCLUSION

In this paper, we propose an *indirect* safe RL method called feasible policy iteration (FPI) that iteratively uses the feasible region of the last policy to constrain the current policy. Our method ensures monotonic expansion of the feasible region and monotonic improvement of the state-value function and is feasible in each iteration. This is achieved by the region-wise feasible policy improvement, which maximizes the return under the constraint of the constraint decay function (CDF) inside the feasible region and minimizes the CDF outside the feasible region. We prove that FPI converges to the maximum feasible region and the optimal state-value function. Experiments on classic control tasks show that FPI achieves zero constraint violations and near-optimal performance. The visualizations of the CDF and state-value function verify the monotonic properties of FPI. Experiments on Safety Gym show that FPI achieves lower constraint violations and comparable or higher performance than the baselines.

REFERENCES

- [1] L. Kaiser, M. Babaeizadeh, P. Milos, B. Osinski, R. H. Campbell, K. Czechowski, D. Erhan, C. Finn, P. Kozakowski, and S. Levine, “Model-based reinforcement learning for atari,” in *International Conference on Learning Representations*, 2020, Conference Proceedings.
- [2] J. Schrittwieser, I. Antonoglou, T. Hubert, K. Simonyan, L. Sifre, S. Schmitt, A. Guez, E. Lockhart, D. Hassabis, T. Graepel, T. Lillicrap, and D. Silver, “Mastering atari, go, chess and shogi by planning with a learned model,” *Nature*, vol. 588, no. 7839, pp. 604–609, 2020. [Online]. Available: <https://doi.org/10.1038/s41586-020-03051-4>
- [3] O. M. Andrychowicz, B. Baker, M. Chociej, R. Jozefowicz, B. McGrew, J. Pachocki, A. Petron, M. Plappert, G. Powell, A. Ray *et al.*, “Learning dexterous in-hand manipulation,” *The International Journal of Robotics Research*, vol. 39, no. 1, pp. 3–20, 2020.
- [4] Y. Guan, Y. Ren, Q. Sun, S. E. Li, H. Ma, J. Duan, Y. Dai, and B. Cheng, “Integrated decision and control: Toward interpretable and computationally efficient driving intelligence,” *IEEE Transactions on Cybernetics*, pp. 1–15, 2022.

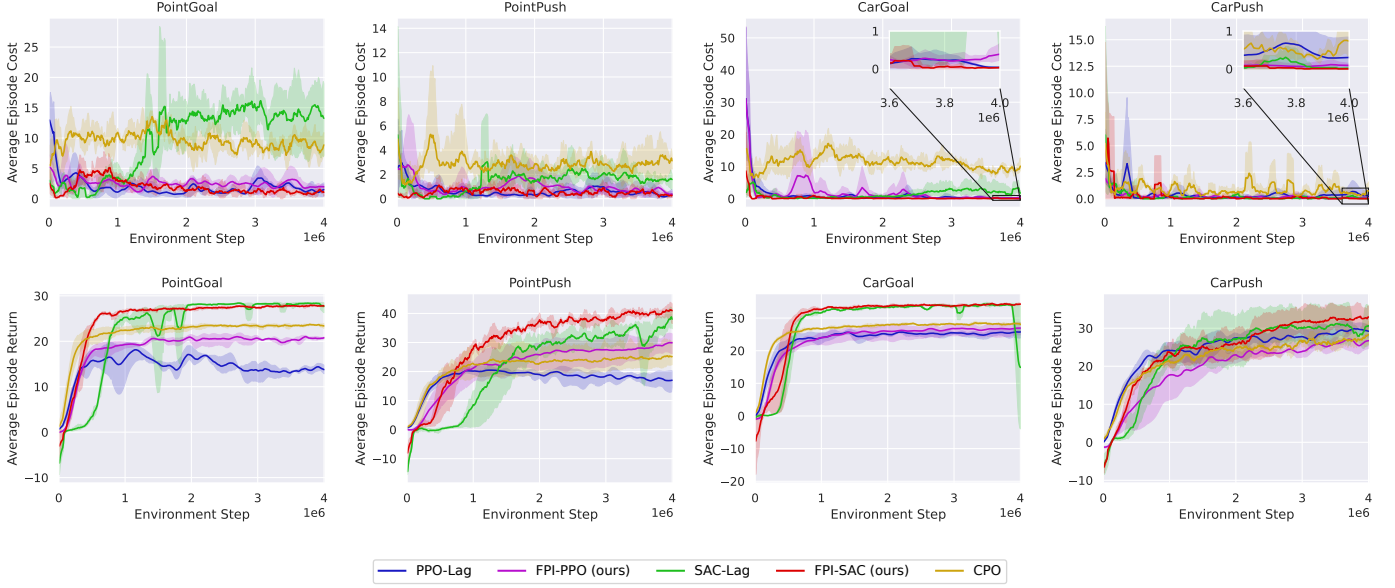


Fig. 4. Training curves on four safety gym tasks. The solid line and the shaded region in each figure correspond to the mean and 95% confidence interval over 3 seeds, respectively. In the first row are the average episode cost curves, and in the second row are the average episode return curves. The columns correspond to the four tasks.

- [5] J. Garcia and F. Fernández, “A comprehensive survey on safe reinforcement learning,” *Journal of Machine Learning Research*, vol. 16, no. 1, pp. 1437–1480, 2015.
- [6] L. Brunke, M. Greeff, A. W. Hall, Z. Yuan, S. Zhou, J. Panerati, and A. P. Schoellig, “Safe learning in robotics: From learning-based control to safe reinforcement learning,” *Annual Review of Control, Robotics, and Autonomous Systems*, vol. 5, pp. 411–444, 2022.
- [7] C. Liu and M. Tomizuka, “Control in a safe set: Addressing safety in human-robot interactions,” in *Dynamic Systems and Control Conference*, vol. 46209. American Society of Mechanical Engineers, 2014, p. V003T42A003.
- [8] A. D. Ames, X. Xu, J. W. Grizzle, and P. Tabuada, “Control barrier function based quadratic programs for safety critical systems,” *IEEE Transactions on Automatic Control*, vol. 62, no. 8, pp. 3861–3876, 2016.
- [9] J. Achiam, D. Held, A. Tamar, and P. Abbeel, “Constrained policy optimization,” in *International Conference on Machine Learning*. PMLR, 2017, Conference Proceedings, pp. 22–31.
- [10] S. Bansal, M. Chen, S. Herbert, and C. J. Tomlin, “Hamilton-jacobi reachability: A brief overview and recent advances,” in *2017 IEEE 56th Annual Conference on Decision and Control (CDC)*. IEEE, 2017, pp. 2242–2253.
- [11] S. Boyd, S. P. Boyd, and L. Vandenberghe, *Convex optimization*. Cambridge university press, 2004.
- [12] Y. Chow, M. Ghavamzadeh, L. Janson, and M. Pavone, “Risk-constrained reinforcement learning with percentile risk criteria,” *The Journal of Machine Learning Research*, vol. 18, no. 1, pp. 6070–6120, 2017.
- [13] C. Tessler, D. J. Mankowitz, and S. Mannor, “Reward constrained policy optimization,” in *International Conference on Learning Representations*, 2019, Conference Proceedings.
- [14] D. Ding, K. Zhang, T. Basar, and M. Jovanovic, “Natural policy gradient primal-dual method for constrained markov decision processes,” *Advances in Neural Information Processing Systems*, vol. 33, pp. 8378–8390, 2020.
- [15] A. Stooke, J. Achiam, and P. Abbeel, “Responsive safety in reinforcement learning by pid lagrangian methods,” in *International Conference on Machine Learning*. PMLR, 2020, pp. 9133–9143.
- [16] S. Paternain, L. Chamon, M. Calvo-Fullana, and A. Ribeiro, “Constrained reinforcement learning has zero duality gap,” *Advances in Neural Information Processing Systems*, vol. 32, 2019.
- [17] M. Yu, Z. Yang, M. Kolar, and Z. Wang, “Convergent policy optimization for safe reinforcement learning,” *Advances in Neural Information Processing Systems*, vol. 32, 2019.
- [18] T.-Y. Yang, J. Rosca, K. Narasimhan, and P. J. Ramadge, “Projection-based constrained policy optimization,” *arXiv preprint arXiv:2010.03152*, 2020.
- [19] T. Haarnoja, A. Zhou, P. Abbeel, and S. Levine, “Soft actor-critic: Off-policy maximum entropy deep reinforcement learning with a stochastic actor,” in *International conference on machine learning*. PMLR, 2018, pp. 1861–1870.
- [20] J. Schulman, P. Wolski, P. Dhariwal, A. Radford, and O. Klimov, “Proximal policy optimization algorithms,” *arXiv preprint arXiv:1707.06347*, 2017.
- [21] A. Ray, J. Achiam, and D. Amodei, “Benchmarking safe exploration in deep reinforcement learning,” *arXiv preprint arXiv:1910.01708*, vol. 7, p. 1, 2019.
- [22] J. Schulman, P. Moritz, S. Levine, M. Jordan, and P. Abbeel, “High-dimensional continuous control using generalized advantage estimation,” *arXiv preprint arXiv:1506.02438*, 2015.
- [23] J. Schulman, S. Levine, P. Abbeel, M. Jordan, and P. Moritz, “Trust region policy optimization,” in *International Conference on Machine Learning*. PMLR, pp. 1889–1897.
- [24] S. Ha, P. Xu, Z. Tan, S. Levine, and J. Tan, “Learning to walk in the real world with minimal human effort,” *arXiv preprint arXiv:2002.08550*, 2020.
- [25] Q. Ge, Q. Sun, S. E. Li, S. Zheng, W. Wu, and X. Chen, “Numerically stable dynamic bicycle model for discrete-time control,” in *2021 IEEE Intelligent Vehicles Symposium Workshops (IV Workshops)*. IEEE, 2021, pp. 128–134.
- [26] G. Brockman, V. Cheung, L. Pettersson, J. Schneider, J. Schulman, J. Tang, and W. Zaremba, “Openai gym,” *arXiv preprint arXiv:1606.01540*, 2016.
- [27] Z. Yuan, A. W. Hall, S. Zhou, L. Brunke, M. Greeff, J. Panerati, and A. P. Schoellig, “safe-control-gym: a unified benchmark suite for safe learning-based control and reinforcement learning,” *arXiv preprint arXiv:2109.06325*, 2021.